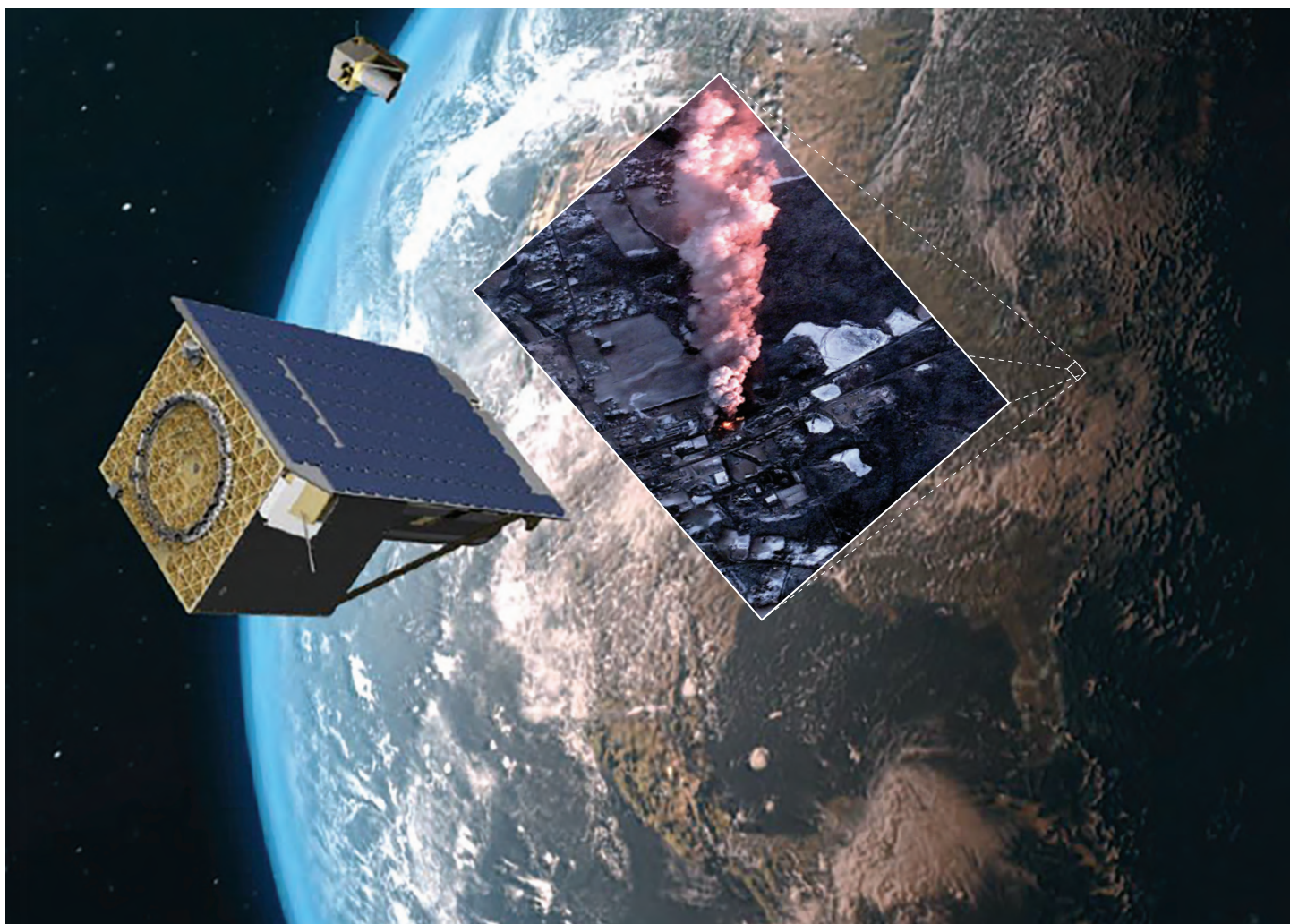


System Characterization Report on the BlackSky Global Multispectral Sensor

Chapter 0 of
System Characterization of Earth Observation Sensors



Open-File Report 2021–1030–0
Version 1.1, April 2024

U.S. Department of the Interior
U.S. Geological Survey

Cover. Image of the BlackSky Global satellite and a satellite image of East Palestine, Ohio, hours after a train carrying hazardous materials burst into flames, taken on February 4, 2023, at 7:32 a.m. local time. Images courtesy of BlackSky, used with permission.

System Characterization Report on the BlackSky Global Multispectral Sensor

By James C. Vrabel,¹ Cody Anderson,² Paul C. Bresnahan,³ Jon B. Christopherson,³ Jeffrey Clauson,³ Minsu Kim,³ Robert E. Ryan,⁴ and Aparajithan Sampath³

Chapter O of

System Characterization of Earth Observation Sensors

Compiled by Shankar N. Ramaseri Chandra³

¹Imaging Technology Consultants, Inc., under contract to the U.S. Geological Survey.

²U.S. Geological Survey.

³KBR, Inc., under contract to the U.S. Geological Survey.

⁴Innovative Imaging & Research, Inc., under contract to the U.S. Geological Survey.

Open-File Report 2021–1030–0
Version 1.1, April 2024

U.S. Department of the Interior
U.S. Geological Survey

U.S. Geological Survey, Reston, Virginia: 2023

First release: 2023

Revised: April 2024 (ver. 1.1)

For more information on the USGS—the Federal source for science about the Earth, its natural and living resources, natural hazards, and the environment—visit <https://www.usgs.gov> or call 1–888–ASK–USGS.

For an overview of USGS information products, including maps, imagery, and publications, visit <https://store.usgs.gov/>.

Any use of trade, firm, or product names is for descriptive purposes only and does not imply endorsement by the U.S. Government.

Although this information product, for the most part, is in the public domain, it also may contain copyrighted materials as noted in the text. Permission to reproduce copyrighted items must be secured from the copyright owner.

Suggested citation:

Vrabel, J.C., Anderson, C., Bresnahan, P.C., Christopherson, J.B., Clauson, J., Kim, M., Ryan, R.E., and Sampath, A., 2023, System characterization report on the BlackSky Global multispectral sensor (ver. 1.1, April 2024), chap. 0 of Ramaseri Chandra, S.N., comp., System characterization of Earth observation sensors: U.S. Geological Survey Open-File Report 2021–1030, 23 p., <https://doi.org/10.3133/ofr202110300>.

ISSN 2331-1258 (online)

Contents

Executive Summary	1
Introduction.....	1
System Description.....	2
Satellite and Operational Details	2
Sensor Information	2
Procedures.....	3
Measurements	3
Analysis	4
Geometric Performance	4
Interior (Band to Band)	4
Exterior (Geometric Location Accuracy)	12
Spatial Performance	16
Summary and Conclusions.....	23
Selected References.....	23

Figures

1. Band 1 to band 2 geometric error map, Baotou, China	5
2. Band 1 to band 2 geometric error histogram, Baotou, China	6
3. Band 1 to band 2 geometric error plot, Baotou, China	6
4. Band 2 to band 3 geometric error map, Baotou, China	7
5. Band 2 to band 3 geometric error plot, Baotou, China	8
6. Band 1 to band 2 geometric error map, Sioux Falls, South Dakota	9
7. Band 1 to band 2 geometric error histogram, Sioux Falls, South Dakota	10
8. Band 1 to band 2 geometric error plot, Sioux Falls, South Dakota	10
9. Band 2 to band 3 geometric error map, Sioux Falls, South Dakota	11
10. Band 2 to band 3 geometric error plot, Sioux Falls, South Dakota	12
11. BlackSky Global orthorectified imagery geometric error plot, Sioux Falls, South Dakota	14
12. BlackSky Global nonorthorectified imagery geometric error plot using affine transform, Sioux Falls, South Dakota	15
13. BlackSky Global nonorthorectified imagery geometric error plot using rational polynomial coefficients, Sioux Falls, South Dakota	16
14. BlackSky image of calibration edge, Baotou, China	17
15. Edge detection, edge spread function plot, line spread function plot and modulation transfer function plot from the image quality estimation algorithm	18
16. BlackSky image of calibration edge, Sioux Falls, South Dakota	19
17. Graphs showing band 1 raw edge transects and shifted transects	20

18. Graphs showing band 1 edge spread function and line spread function and modulation transfer function20

19. Graphs showing band 2 raw edge transects and shifted transects21

20. Graphs showing band 2 edge spread function and line spread function and modulation transfer function21

21. Graphs showing band 3 raw edge transects and shifted transects22

22. Graphs showing band 3 edge spread function and line spread function and modulation transfer function22

Tables

1. Satellite and operational details for the BlackSky Global SpaceView-24 multispectral sensor.....2

2. Imaging sensor details for BlackSky Global satellites 9 and 12–173

3. U.S. Geological Survey measurement results4

4. Band-to-band registration error.....5

5. BlackSky Global images assessed over Sioux Falls, South Dakota13

6. Geometric error of BlackSky Global orthorectified imagery relative to ground-surveyed control points.....13

7. Geometric error of BlackSky Global nonorthorectified imagery relative to ground-surveyed control points using affine transform14

8. Geometric error of BlackSky Global nonorthorectified imagery relative to ground-surveyed control points using rational polynomial coefficients.....15

9. Spatial performance of the BlackSky Global SpaceView-24 multispectral sensor using an image quality estimation algorithm17

10. Spatial performance of the BlackSky Global SpaceView-24 multispectral sensor using Innovative Imaging & Research, Inc., Image Quality Estimation software18

11. Spatial performance of the BlackSky Global SpaceView-24 multispectral sensor using U.S. Geological Survey Earth Resources Observation and Science system characterization software18

Conversion Factors

International System of Units to U.S. customary units

Multiply	By	To obtain
Length		
centimeter (cm)	0.3937	inch (in.)
meter (m)	3.281	foot (ft)
meter (m)	1.094	yard (yd)
kilometer (km)	0.6214	mile (mi)
Mass		
kilogram (kg)	2.205	pound avoirdupois (lb)

Abbreviations

ECCOE	Earth Resources Observation and Science Cal/Val Center of Excellence
ESF	edge spread function
FWHM	full width at half maximum
GSD	ground sample distance
IQE	Image Quality Estimation
JACIE	Joint Agency Commercial Imagery Evaluation
MTF	modulation transfer function
NSSDA	National Standard for Spatial Data Accuracy
RPC	rational polynomial coefficient
USGS	U.S. Geological Survey

System Characterization Report on the BlackSky Global Multispectral Sensor

By James C. Vrabel,¹ Cody Anderson,² Paul C. Bresnahan,³ Jon B. Christopherson,³ Jeffrey Clauson,³ Minsu Kim,³ Robert E. Ryan,⁴ and Aparajithan Sampath³

Executive Summary

This report addresses system characterization of the BlackSky Global satellites and is part of a series of system characterization reports produced and delivered by the U.S. Geological Survey Earth Resources Observation and Science Cal/Val Center of Excellence. These reports present and detail the methodology and procedures for characterization; present technical and operational information about the specific sensing system being evaluated; and provide a summary of test measurements, data retention practices, data analysis results, and conclusions.

The BlackSky Global satellites are three-band multispectral imagers (red, green, and blue multispectral bands plus a panchromatic band) with a 0.8- to 0.9-meter (m) pixel ground sample distance for the assessed satellites. BlackSky Global satellites 9 and 12–17 were launched in March and December 2021, respectively, into a Sun-synchronous orbit of 430–450 kilometers with an inclination of 42–53 degrees and a swath width of 6 kilometers at nadir. Each Global satellite has an expected lifetime of about 3 years. More information on the BlackSky Global satellites is available in the “Land Remote Sensing Satellites Online Compendium” (<https://calval.cr.usgs.gov/apps/compendium>) and from BlackSky at www.BlackSky.com.

The Earth Resources Observation and Science Cal/Val Center of Excellence system characterization team completed data analyses to characterize the geometric (interior and exterior) and spatial performances. Results of these analyses indicate that the assessed BlackSky Global satellites have an interior geometric performance in the range of –0.011 m (–0.012 pixel) to 0.007 m (0.008 pixel) in easting and –0.018 m (–0.020 pixel) to 0.012 m (0.013 pixel) in northing in band-to-band registration; an exterior geometric

performance using ground control points of 8.0-m circular error (95-percent certainty) for orthorectified products and 8.8- to 14.3-m circular error (95-percent certainty) for non-orthorectified products, depending on the geolocation metadata used; and a spatial performance in the range of 1.70 to 2.43 pixels for full width at half maximum, with a modulation transfer function at a Nyquist frequency in the range of 0.032 to 0.084.

Introduction

The SpaceView-24 camera sensor onboard the BlackSky Global satellites is a high-resolution land observation instrument that can measure the Earth’s radiation in three multispectral bands (blue, green, and red) and a panchromatic band. The BlackSky Global satellites assessed in this report were all launched in 2021. BlackSky Global satellites 9 and 12–17 were launched in March and December 2021, respectively, into a Sun-synchronous orbit of 430–450 kilometers with an inclination of 42–53 degrees and a swath width of 6 kilometers at nadir. Each Global satellite has an expected lifetime of about 3 years. The SpaceView-24 camera has an aperture of 24 centimeters and collects imagery at ground resolutions between 0.8 and 0.9 meter (m) for the assessed satellites. The satellites are developed by Spaceflight Industries for BlackSky. More information on the BlackSky Global satellites and the sensor is available in the “Land Remote Sensing Satellites Online Compendium” (<https://calval.cr.usgs.gov/apps/compendium>) and from BlackSky at www.BlackSky.com.

The data analysis results provided in this report have been derived from approved Joint Agency Commercial Imagery Evaluation (JACIE) processes and procedures. JACIE was formed to leverage resources from several Federal agencies for the characterization of remote sensing data and to share those results across the remote sensing community. More information about JACIE is available at <https://www.usgs.gov/calval/jacie>.

The purpose of this report is to describe the specific sensor or sensing system, test its performance in two categories, complete related data analyses to quantify these performances, and report the results in a standardized document. In this

¹Imaging Technology Consultants, Inc., under contract to the U.S. Geological Survey.

²U.S. Geological Survey.

³KBR, Inc., under contract to the U.S. Geological Survey.

⁴Innovative Imaging & Research, Inc., under contract to the U.S. Geological Survey.

chapter, the BlackSky Global sensor is described. The performance testing of the system is limited to geometric and spatial qualities. The scope of the geometric assessment is limited to testing the interior alignments of spectral bands against each other. The exterior alignment is tested in reference to surveyed ground control points.

Most of the U.S. Geological Survey (USGS) system characterization reports also assess the radiometric accuracy of a sensor. However, the Global SpaceView-24 sensor collects color imagery optimized for visual analysis and not radiometric analysis based on customer requirements. Therefore, the sensor is not a radiometric product and a radiometric accuracy assessment was not necessary.

The USGS Earth Resources Observation and Science Cal/Val Center of Excellence (ECCOE) project, and the associated system characterization process used for this assessment, follows the USGS Fundamental Science Practices, which include maintaining data, information, and documentation needed to reproduce and validate the scientific analysis documented in this report. Additional information and guidance about Fundamental Science Practices and related resource information of interest to the public are available at <https://www.usgs.gov/about/organization/science-support/office-science-quality-and-integrity/fundamental-science-practices>. For additional information related to the report, please contact ECCOE at eccoe@usgs.gov.

This section describes the satellite and operational details and provides information about the BlackSky Global SpaceView-24 sensor.

System Description

This section describes the satellite and operational details and provides information about the BlackSky Global SpaceView-24 sensor.

Satellite and Operational Details

The satellite and operational details for the BlackSky Global satellites are listed in [table 1](#).

Sensor Information

The imaging sensor details for the SpaceView-24 camera are listed in [table 2](#).

Table 1. Satellite and operational details for the BlackSky Global SpaceView-24 multispectral sensor.

[kg, kilogram; km, kilometer; °, degree; ~, about; m, meter]

Product information		BlackSky Global satellite	
Satellite and operational information			
Product name	BlackSky On-Demand (orthorectified or nonorthorectified product)		
Satellite name	Global 9, 16, 17 (assessed)		
Satellite mass	56 kg		
Sensor name	SpaceView-24		
Sensor type	Multispectral (red, green, blue, panchromatic)		
Mission type	Global monitoring		
Launch dates	March 22, 2021–December 9, 2021 (for assessed satellites)		
Number of satellites	15 (constellation total)		
Expected lifetime	3 years		
Operator	BlackSky		
Operational details			
Operating orbit	Sun-synchronous orbit		
Orbital altitude	430–450 km		
Orbital inclination	42–53°		
Temporal coverage	December 2018 to present (2023)		
Imaging angles	~30° off nadir		
Ground sample distance	0.8–0.9 m (for the assessed Global satellites)		
Swath width	6 km		
Website	www.blacksky.com		

Table 2. Imaging sensor details for BlackSky Global satellites 9 and 12–17.[μm , micrometer; m, meter]

Spectral band details	BlackSky SpaceView-24			
	Lower band (μm)	Upper band (μm)	Radiometric resolution (bits)	Ground sample distance (m)
Band 1—red	0.59	0.70	12	0.8–0.9
Band 2—green	0.50	0.59	12	0.8–0.9
Band 3—blue	0.45	0.50	12	0.8–0.9

Procedures

ECCOE has established standard processes to identify Earth observing systems of interest and to assess the geometric, radiometric (not completed for this assessment), and spatial qualities of data products from these systems.

The assessment steps are as follows:

- system identification and investigation to learn the general specifications of the satellite and its sensor(s);
- data receipt and initial inspection to understand the characteristics and any overt flaws in the data product so that it may be further analyzed;
- geometric characterization, including interior geometric orientation measuring the relative alignment of spectral bands and exterior geometric orientation measuring how well the georeferenced pixels within the image are aligned to a known reference;

- radiometric characterization (not completed for this assessment), including assessing how well the data product correlates with a known reference and, when possible, assessing the signal-to-noise ratio; and
- spatial characterization, assessing the two-dimensional fidelity of the image pixels to their projected ground sample distance (GSD).

Data analysis and test results are maintained at the USGS Earth Resources Observation and Science Center by the ECCOE project.

Measurements

The observed USGS measurements are listed in [table 3](#). Details about the methodologies used are outlined in the “Analysis” section.

Table 3. U.S. Geological Survey measurement results.

[m, meter; RMSE, root mean square error; GCP, ground control point; %, percent; RPC, rational polynomial coefficient; FWHM, full width at half maximum; RER, relative edge response; MTF, modulation transfer function; USGS, U.S. Geological Survey; EROSSC, Earth Resources Observation and Science system characterization; JSON, JavaScript Object Notation; GSD, ground sample distance]

Description of product	Orthorectified and nonorthorectified (digital numbers)
Geometric performance ranges (easting, northing), in meters (pixels ¹)	
Interior (band to band)	All bands combined to reference band 2 (green) Mean: −0.011 to 0.007 m (−0.012 to 0.008), −0.018 to 0.012 m (−0.020 to 0.013) RMSE: 0.019 to 0.059 m (0.021 to 0.066), 0.014 to 0.067 m (0.016 to 0.074)
Exterior (geometric location accuracy compared to GCPs)	Nonorthorectified (affine ²) Circular error: 14.3 m (95%) Nonorthorectified (RPC) Circular error: 8.8 m (95%) Orthorectified Circular error: 8.0 m (95%)
Spatial performance (FWHM, RER, MTF at Nyquist)	
Spatial performance measurement (image quality estimation algorithms [Helder and others, 2003; Innovative Imaging & Research, Inc., 2018])	Band 1 across track: 2.13–2.25 pixels, 0.40–0.42, 0.032–0.050 Band 1 along track: 1.94–2.06 pixels, 0.40–0.44, 0.050–0.080 Band 2 across track: 2.01–2.03 pixels, 0.42–0.43, 0.040–0.060 Band 2 along track: 1.85–1.99 pixels, 0.41–0.46, 0.050–0.060 Band 3 across track: 1.97–2.09 pixels, 0.43–0.43, 0.047–0.050 Band 3 along track: 1.70–1.98 pixels, 0.47–0.49, 0.080–0.084
Spatial performance measurement (USGS EROSSC)	Band 1: 2.43 pixels, 0.36, 0.045 Band 2: 2.35 pixels, 0.38, 0.060 Band 3: 2.25 pixels, 0.41, 0.074
Known artifacts and quality issues	
USGS noted artifacts/quality issues	The JSON file always indicates that a product is orthorectified even when it is not orthorectified. This was verified by checking the JSON files of six nonorthorectified scenes.

¹Pixel values are provided at a 0.9-m GSD for interior assessment and a 0.8- to 0.9-m GSD for exterior geometric assessment.

²A two-dimensional affine transformation was applied to the data. Affine enables skew in addition to rotation, translation, and scale; that is, the x- and y-axes can rotate differently, or x and y can have different scales, causing the skew effect.

Analysis

This section of the report describes the geometric and spatial performance of the BlackSky Global satellites.

Geometric Performance

The geometric performance for the BlackSky Global satellites is characterized in terms of the interior (band-to-band alignment) and exterior (geometric location accuracy) geometric analysis results. Interior accuracy measures how well the various bands of the BlackSky Global satellites are aligned to each other. Exterior accuracy measures the geometric location accuracy of the BlackSky Global satellites compared to surveyed USGS ground control points. Together, the interior and exterior geometric analysis results, as reported in the “Interior (Band to Band)” and “Exterior (Geometric Location Accuracy)” sections, provide a comprehensive assessment of geometric accuracy.

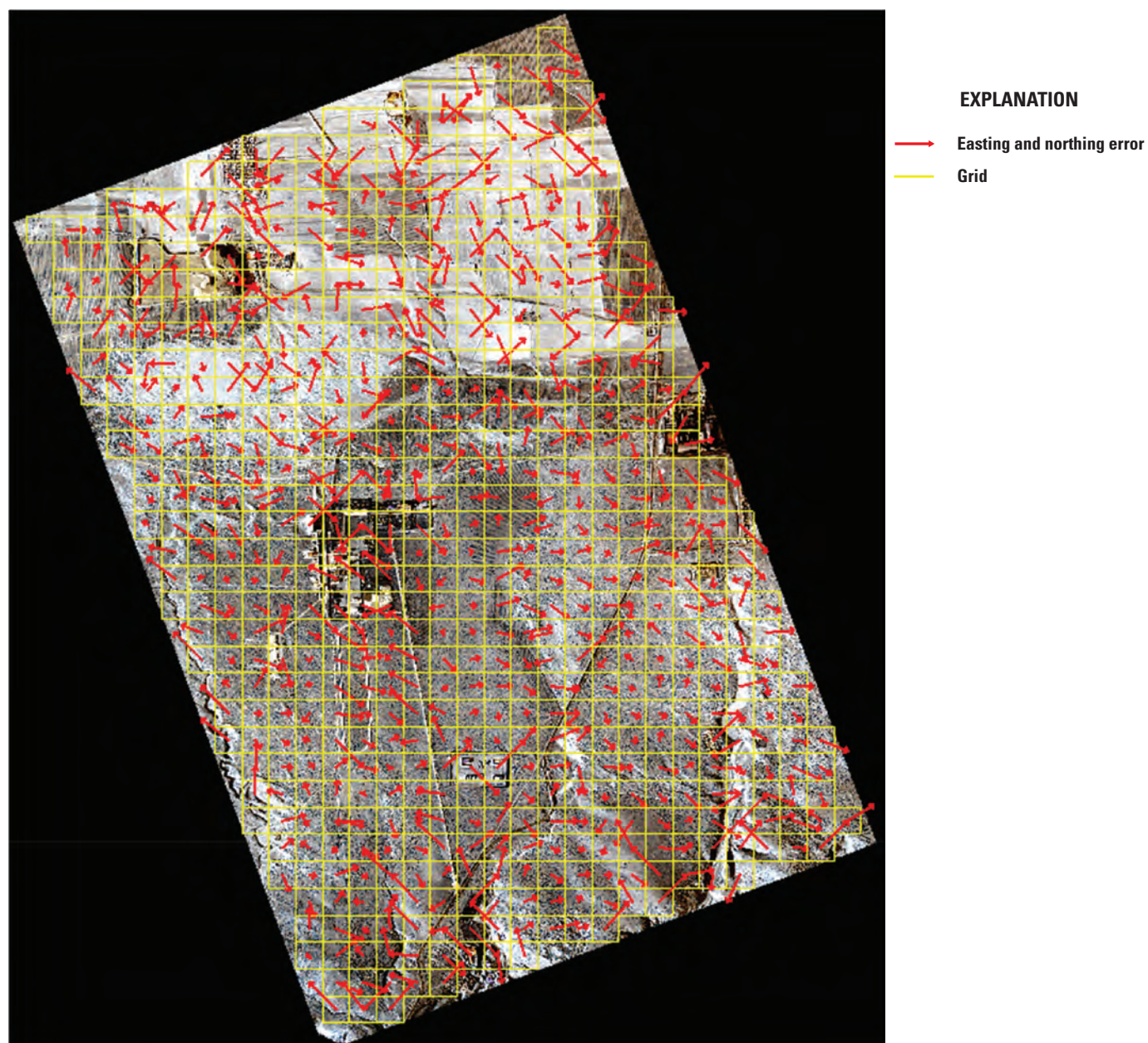
Interior (Band to Band)

The band-to-band alignment analysis was completed using the Earth Resources Observation and Science system characterization software on two images over Baotou, China, and Sioux Falls, South Dakota. Orthorectified products were assessed for band-to-band alignment based on customer requirements. Band combinations were registered against each other to determine the mean error and root mean square error, as listed in [table 4](#), with results represented in pixels at a 0.9-m GSD. Results of band comparisons to the green band are provided. Geometric error maps for each green band comparison over the two scenes, as well as the corresponding error plots, are shown in [figures 1–10](#). Geometric error histogram graphs also are shown for the green-to-blue band comparisons for each of the scenes. The geometric error maps indicate the directional shift and relative magnitude of the shift, and the histogram graphs indicate the frequency of observed mean error measurements within the image. The geometric error plots indicate the easting and northing errors between the designated bands.

Table 4. Band-to-band registration error (in pixels).

[Band 1 is red, band 2 is green, and band 3 is blue. RMSE, root mean square error]

Scene identifiers	Band combination	Mean error (easting)	Mean error (northing)	RMSE (easting)	RMSE (northing)
BSG-113-20220304-073320-20006184_ortho (Baotou, China)	Band 2–band 1	0.008	−0.002	0.028	0.027
	Band 2–band 3	−0.012	−0.006	0.021	0.016
BSG-113-20220708-143244-29957204_ortho (Sioux Falls, South Dakota)	Band 2–band 1	0	−0.020	0.051	0.057
	Band 2–band 3	0.008	0.013	0.066	0.074

**Figure 1.** Band 1 (red) to band 2 (green) geometric error map, Baotou, China.

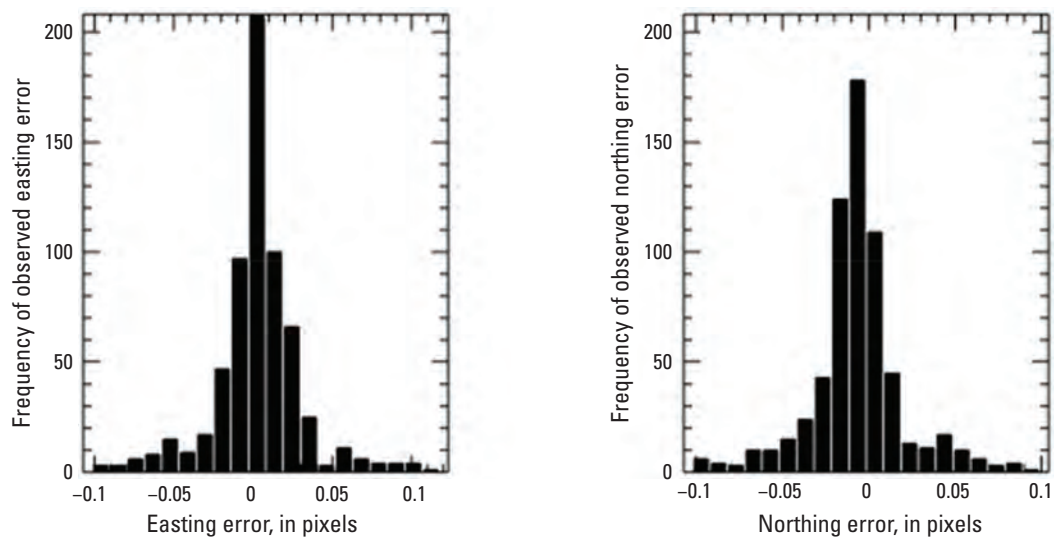


Figure 2. Band 1 (red) to band 2 (green) geometric error histogram, Baotou, China.

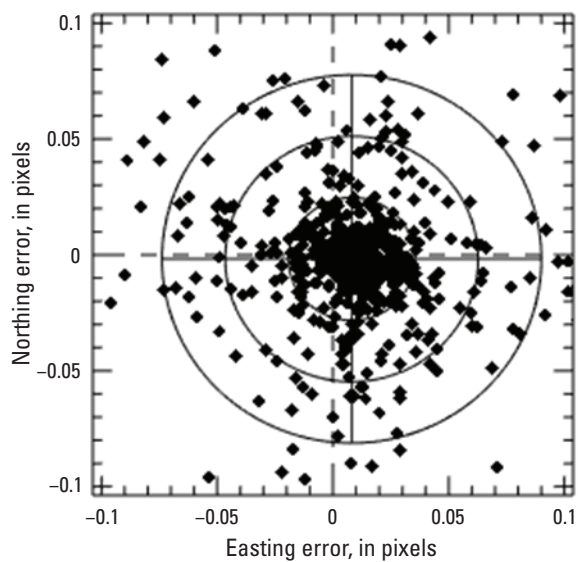


Figure 3. Band 1 (red) to band 2 (green) geometric error plot, Baotou, China.

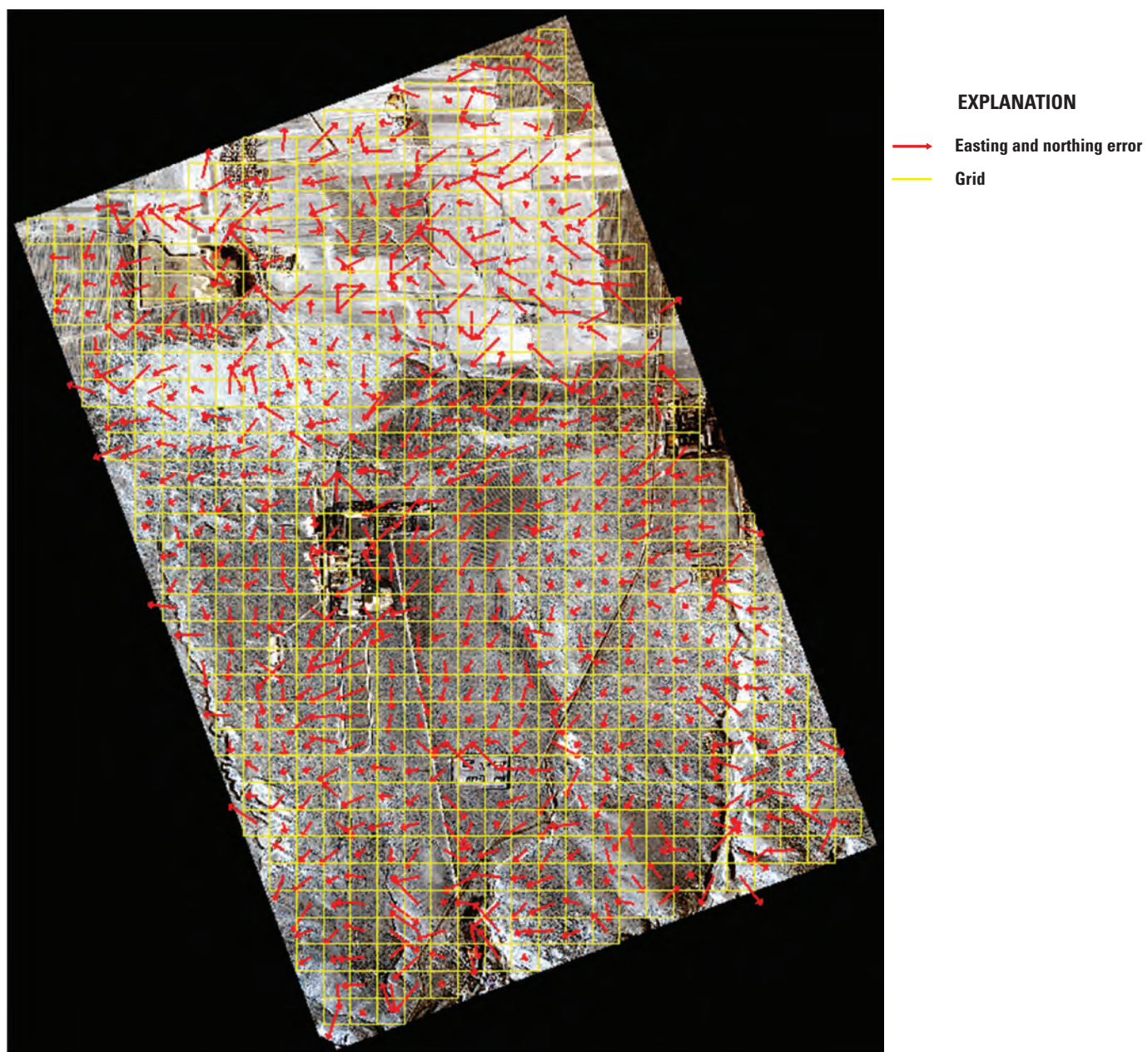


Figure 4. Band 2 (green) to band 3 (blue) geometric error map, Baotou, China.

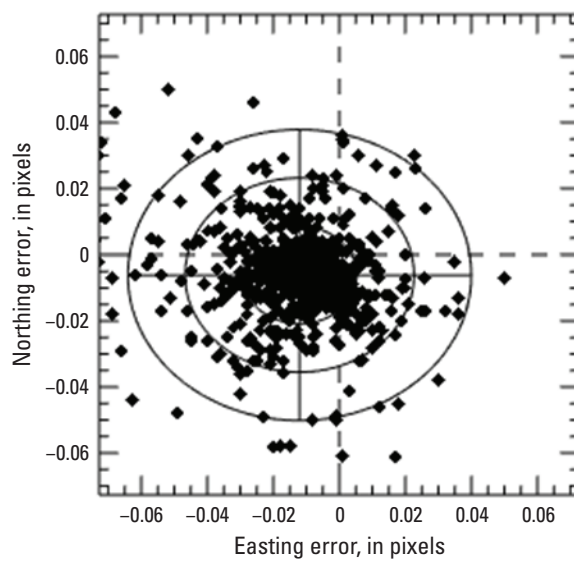


Figure 5. Band 2 (green) to band 3 (blue) geometric error plot, Baotou, China.

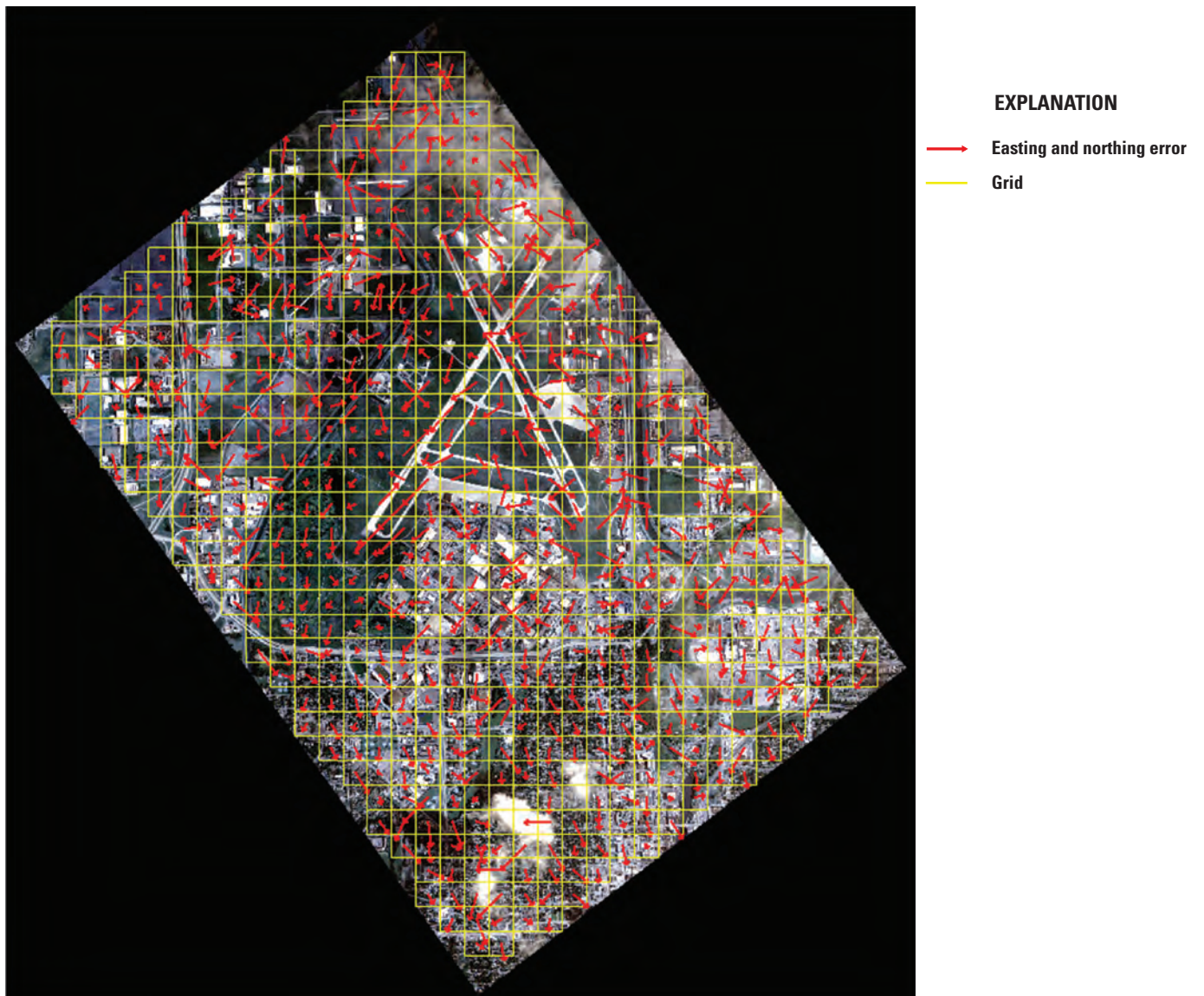


Figure 6. Band 1 (red) to band 2 (green) geometric error map, Sioux Falls, South Dakota.

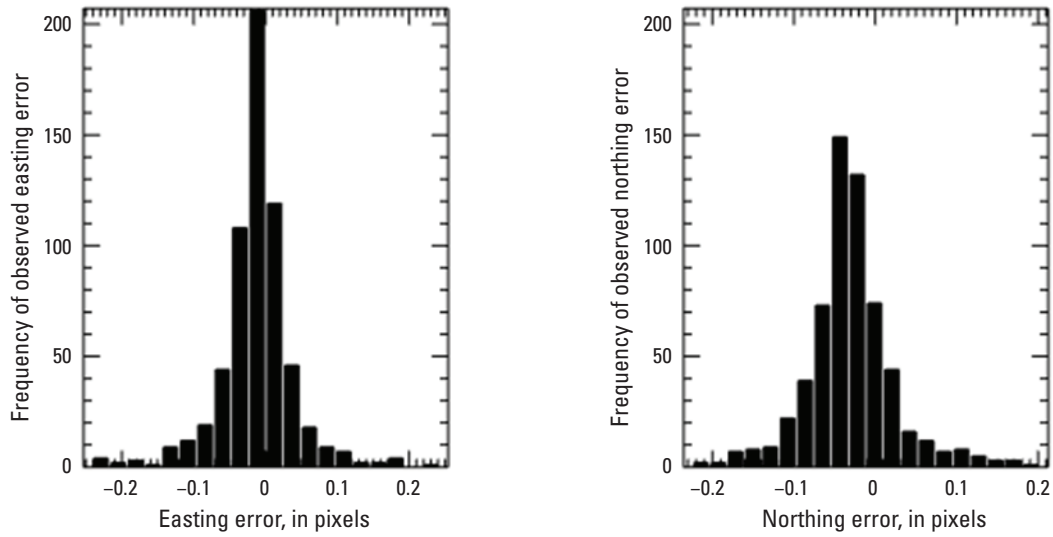


Figure 7. Band 1 (red) to band 2 (green) geometric error histogram, Sioux Falls, South Dakota.

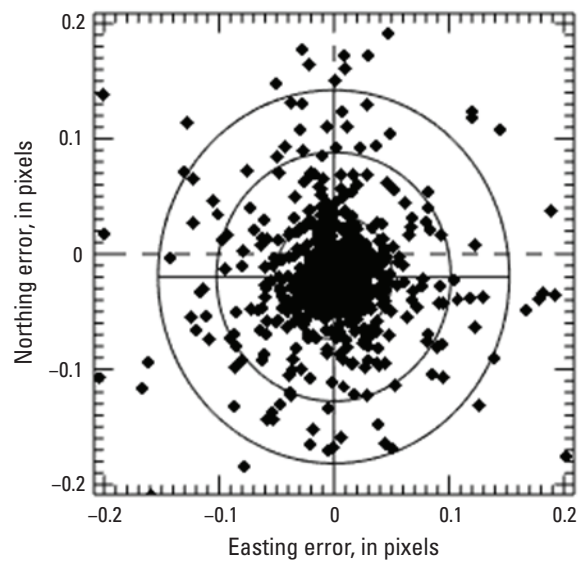


Figure 8. Band 1 (red) to band 2 (green) geometric error plot, Sioux Falls, South Dakota.

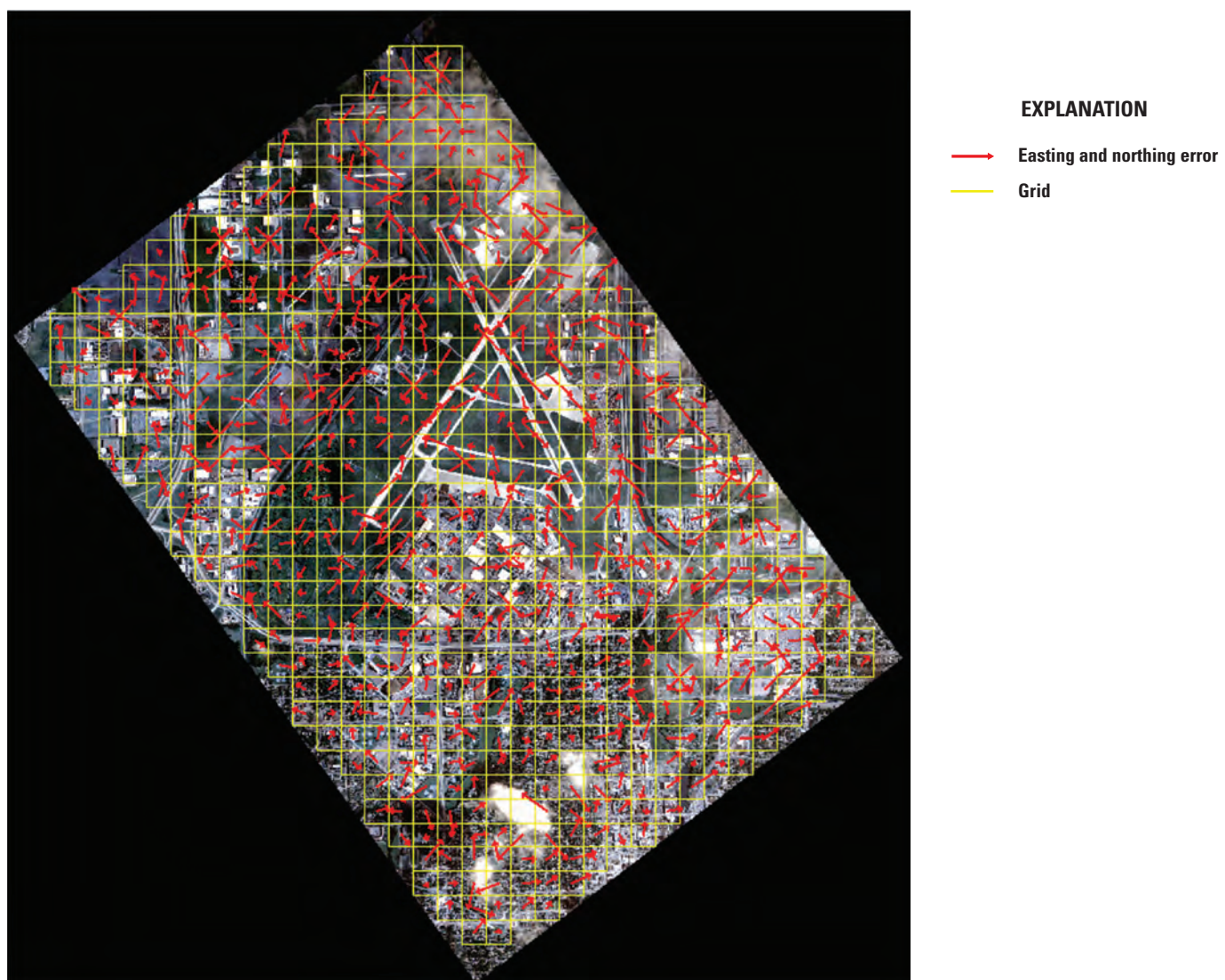


Figure 9. Band 2 (green) to band 3 (blue) geometric error map, Sioux Falls, South Dakota.

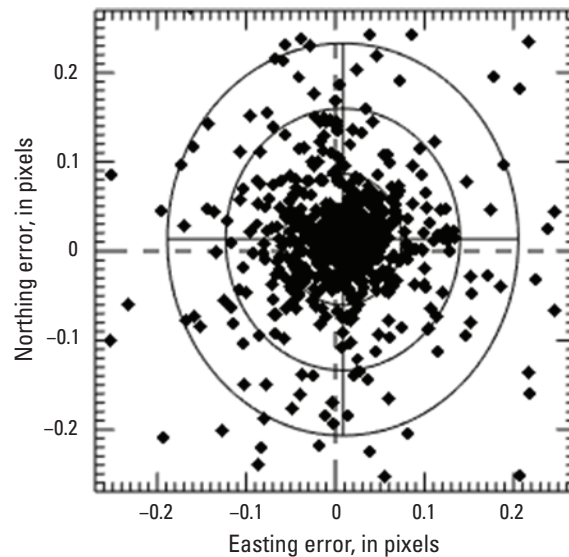


Figure 10. Band 2 (green) to band 3 (blue) geometric error plot, Sioux Falls, South Dakota.

Exterior (Geometric Location Accuracy)

For this analysis, 13 ground-surveyed control points over Sioux Falls, S. Dak., were manually measured using the QGIS open-source software (formerly known as Quantum Geographic Information System software) on three separate BlackSky Global three-band images. The images assessed have a nominal GSD of 0.9-m and are listed in [table 5](#). Each image was processed as an orthorectified image and a non-orthorectified, perspective-geometry image and stored in the GeoTIFF image format.

Geolocation for the orthorectified images was based on the World Geodetic System of 1984 Universal Transverse Mercator Zone 14 north projection (European Petroleum Survey Group code 32614) stored in the GeoTIFF. Two geolocation options were available for the nonorthorectified images. The first was an affine transform stored in the GeoTIFF that relates any pixel location to World Geodetic System of 1984 latitude and longitude coordinates (European Petroleum Survey Group code 4326). The second was a two-dimensional image pixel to three-dimensional World Geodetic System of 1984 geodetic latitude, longitude, and ellipsoid height transform based on a pair of rational polynomial functions. The unique transform parameters for each nonorthorectified image, including the rational polynomial coefficients (RPCs), are stored in a text file with “_rpc.txt” appended to the base name of the corresponding image. Geospatial software packages that use RPC data will typically recognize the presence of the RPC text file accompanying the GeoTIFF and then use the RPCs for geolocation in lieu of the affine transform stored

within the GeoTIFF. QGIS does not use RPCs and thus uses the affine transform. To assess geolocation using RPCs, pixel coordinates measured using QGIS were used with the ellipsoid height of each ground-surveyed point to determine horizontal ground coordinates using an image-to-ground inversion of the rational polynomial functions implemented in separate Python code.

Three geolocation accuracy assessments were completed: (1) orthorectified images using the Universal Transverse Mercator projection defined in the GeoTIFF, (2) nonorthorectified images using the affine transform defined in the GeoTIFF, and (3) nonorthorectified images using the RPCs stored in the separate text file. Measurements from all three images were combined for each assessment. Each set of horizontal coordinates derived from an image pixel was compared to the known set of horizontal coordinates of the corresponding ground-surveyed control point to determine the horizontal errors for that point.

Error statistics for the orthorectified images are listed in [table 6](#), and an error plot is provided in [figure 11](#). The National Standard for Spatial Data Accuracy (NSSDA) metric, which is a 95-percent circular error value, is 8.0 m.

Error statistics for the nonorthorectified images based on the affine transform are listed in [table 7](#), and an error plot is provided in [figure 12](#). The NSSDA metric, which is a 95-percent circular error value, is 14.3 m.

Error statistics for the nonorthorectified images based on RPCs are listed in [table 8](#), and an error plot is provided in [figure 13](#). The NSSDA metric, which is a 95-percent circular error value, is 8.8 m.

Table 5. BlackSky Global images assessed over Sioux Falls, South Dakota.

Scene identifiers	Collection date (month/day/year)
BSG-109-20220125-153823-18123850	1/25/2022
BSG-109-20220514-180301-24140857	5/14/2022
BSG-113-20220708-143244-29957204	7/8/2022

Table 6. Geometric error of BlackSky Global orthorectified imagery relative to ground-surveyed control points.

[SDDEV, standard deviation; RMSE, root mean square error; NSSDA, National Standard for Spatial Data Accuracy; %, percent; m, meter; ~, about; pix, pixel]

Scene identifiers	Mean error (easting)	Mean error (northing)	SDDEV (easting)	SDDEV (northing)	RMSE error (easting)	RMSE error (northing)	NSSDA (95% circular error value)
BSG-109-20220125-153823-18123850, BSG-109-20220514-180301-24140857, and BSG-113-20220708-143244-29957204 (Sioux Falls, South Dakota)	2.9 m (~3.2 pix)	-1.1 m (~1.2 pix)	2.5 m (~2.8 pix)	2.4 m (~2.7 pix)	3.8 m (~4.2 pix)	2.6 m (~2.9 pix)	8.0 m (~8.9 pix)

It is apparent in the nonorthorectified imagery assessment results that geolocation is more accurate using the RPC data than using the affine transform stored in the GeoTIFF. Unlike the RPC model, an affine transform cannot fully model the three-dimensional perspective projection of a

nonorthorectified image. Users should be aware that some software packages will automatically use the affine transform and that better geolocation will result with software that uses RPC with nonorthorectified images.

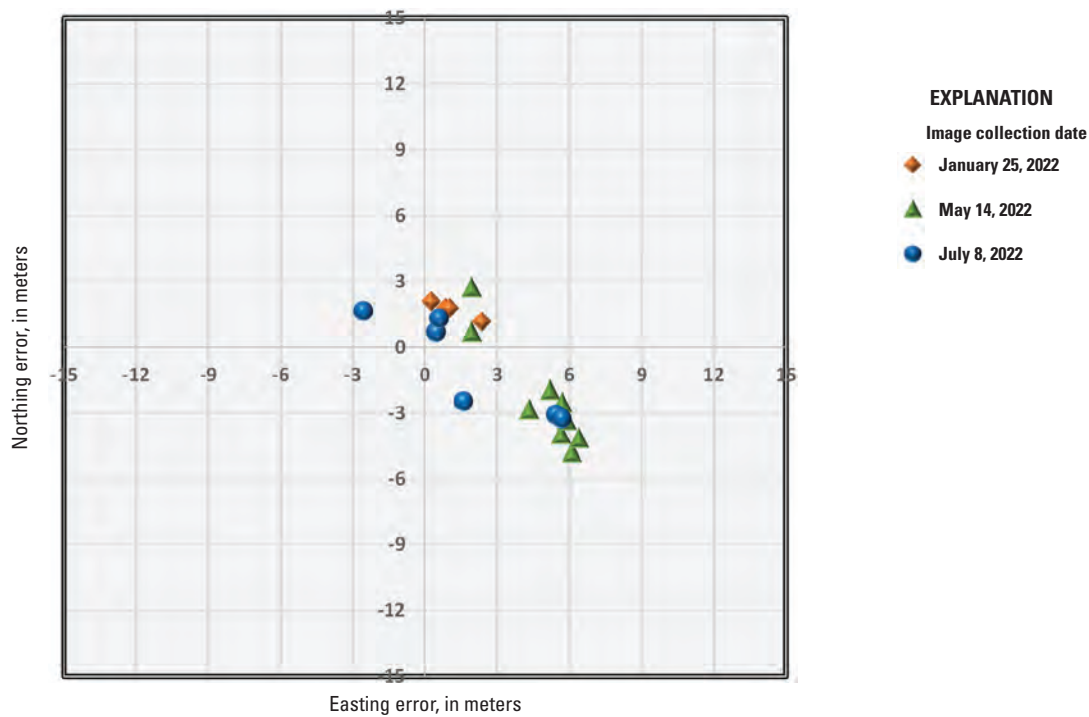


Figure 11. BlackSky Global orthorectified imagery geometric error plot, Sioux Falls, South Dakota.

Table 7. Geometric error of BlackSky Global nonorthorectified imagery relative to ground-surveyed control points using affine transform.

[SDDEV, standard deviation; RMSE, root mean square error; NSSDA, National Standard for Spatial Data Accuracy; %, percent; m, meter; ~, about; pix, pixel]

Scene identifiers	Mean error (easting)	Mean error (northing)	SDDEV (easting)	SDDEV (northing)	RMSE error (easting)	RMSE error (northing)	NSSDA (95% circular error value)
BSG-109-20220125-153823-18123850, BSG-109-20220514-180301-24140857, and BSG-113-20220708-143244-29957204 (Sioux Falls, South Dakota)	3.9 m (~4.3 pix)	-1.3 m (~1.4 pix)	4.7 m (~5.2 pix)	5.7 m (~6.3 pix)	6.0 m (~6.7 pix)	5.7 m (~6.3 pix)	14.3 m (~15.9 pix)

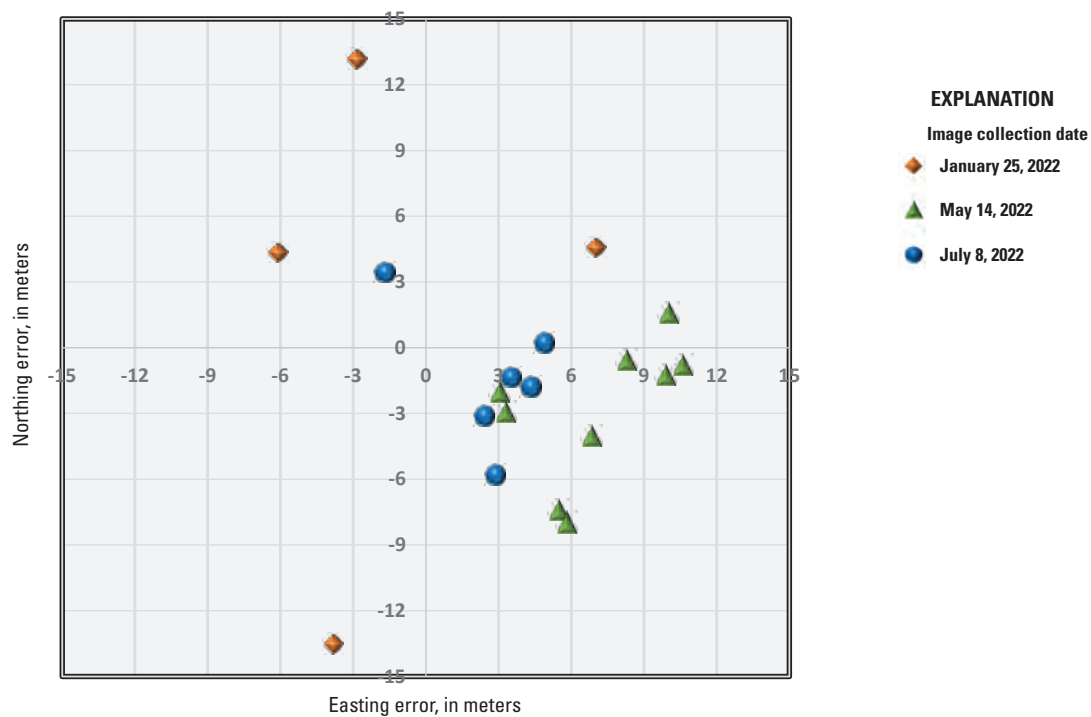


Figure 12. BlackSky Global nonorthorectified imagery geometric error plot using affine transform, Sioux Falls, South Dakota.

Table 8. Geometric error of BlackSky Global nonorthorectified imagery relative to ground-surveyed control points using rational polynomial coefficients.

[SDDEV, standard deviation; RMSE, root mean square error; NSSDA, National Standard for Spatial Data Accuracy; %, percent; m, meter; ~, about; pix, pixel]

Scene identifiers	Mean error (easting)	Mean error (northing)	SDDEV (easting)	SDDEV (northing)	RMSE error (easting)	RMSE error (northing)	NSSDA (95% circular error value)
BSG-109-20220125-153823-18123850,	2.9 m	-2.3 m	2.4 m	2.6 m	3.7 m	3.5 m	8.8 m
BSG-109-20220514-180301-24140857, and	(~3.2 pix)	(~2.6 pix)	(~2.7 pix)	(~2.9 pix)	(~4.1 pix)	(~3.9 pix)	(~9.8 pix)
BSG-113-20220708-143244-29957204 (Sioux Falls, South Dakota)							

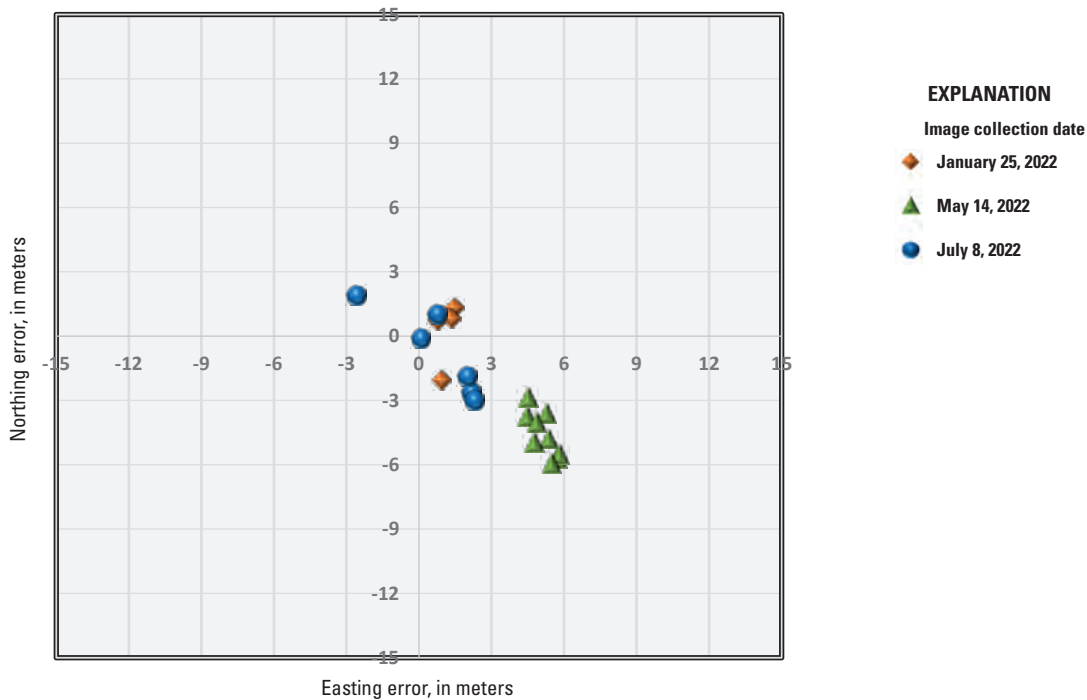


Figure 13. BlackSky Global nonorthorectified imagery geometric error plot using rational polynomial coefficients, Sioux Falls, South Dakota.

Spatial Performance

For this analysis, three methods were used. The first method, an image quality estimation algorithm using point spread functions, based on Helder and others (2003), was used to determine the relative edge response, full width at half maximum (FWHM), and modulation transfer function (MTF) at Nyquist frequency, as listed in [table 9](#). A Global-13 scene of Baotou, China (BSG-113-20220304-073320-20006184_ortho), was used for the spatial assessment (this software required the use of the Baotou site engineered edge targets within the scene) and is shown in [figure 14](#). Orthorectified scenes were used for the spatial performance tests based on customer requirements. The metrics in [table 9](#) were produced from the average results from multiple edges (4–8) within each of the three bands. Along-track and across-track results are presented. The plots in [figure 15](#) represent a typical result for one of the edges identified by the algorithm. The plots show the edge target at Baotou ([fig. 14](#)) and the derived edge spread function (ESF) using a Fermi curve fit and the line spread function, as well as the MTF curve. The ESF plot shows pixel values normalized between 0 and 1 on the y-axis and a blue curve (Fermi) fitted to the red dots as we move across the black-white edge. The line spread function is the mathematical derivative of the ESF and is used to estimate the FWHM.

The second spatial analysis method applied used the Image Quality Estimation (IQE) software from Innovative Imaging & Research, Inc (commonly referred to as I2R). As

stated in the IQE user’s guide, the IQE software is an automated “tool that can estimate the spatial resolution performance of an image product by finding, selecting, and using uniform, high-contrast edges that normally occur within many acquired scenes” (Innovative Imaging & Research, Inc., 2018, p. 1). The IQE software also estimated the relative edge response, FWHM, and MTF at Nyquist frequency. The IQE software was applied to a BlackSky Global-13 scene of Sioux Falls (BSG-113-20220304-073320-20006184_ortho) for this spatial assessment, and the results are listed in [table 10](#). The Sioux Falls scene was used here because the IQE software required a scene where more suitable edges can be identified.

The third method involved the USGS Earth Resources Observation and Science system characterization software. For this analysis, the ESF and line spread function were calculated with resulting FWHM and MTF at Nyquist frequency analysis outputs, as listed in [table 11](#). An edge from a Sioux Falls scene (BSG-109-20220514-180301-24140857_georeferenced.tif) was used, as shown in [figure 16](#), and includes the edge transect bounding box. The results for band 1 are shown in [figures 17 and 18](#). In [figure 17](#), the raw transect is shown in the upper plot. The lower plot in [figure 17](#) shows the shifted transect. The upper plot in [figure 18](#) shows an ESF with the relative edge response and a line spread function with a line segment representing FWHM. The lower plot in [figure 18](#) shows an MTF up to Nyquist frequency (0.5) and the frequency corresponding to the 50-percent MTF value. The results for band 2 are shown in [figures 19 and 20](#), and the results for band 3 are shown in [figures 21 and 22](#).

Table 9. Spatial performance of the BlackSky Global SpaceView-24 multispectral sensor using an image quality estimation algorithm (based on Helder and others [2003]).

[RER, relative edge response; FWHM, full width at half maximum; MTF, modulation transfer function; %, percent]

Spatial analysis	RER		FWHM (pixels)		MTF at Nyquist (%)	
	Along	Across	Along	Across	Along	Across
Band 1—red	0.44	0.40	1.94	2.13	5.0	3.2
Band 2—green	0.46	0.42	1.85	2.03	6.0	4.0
Band 3—blue	0.49	0.43	1.70	1.97	8.4	4.7

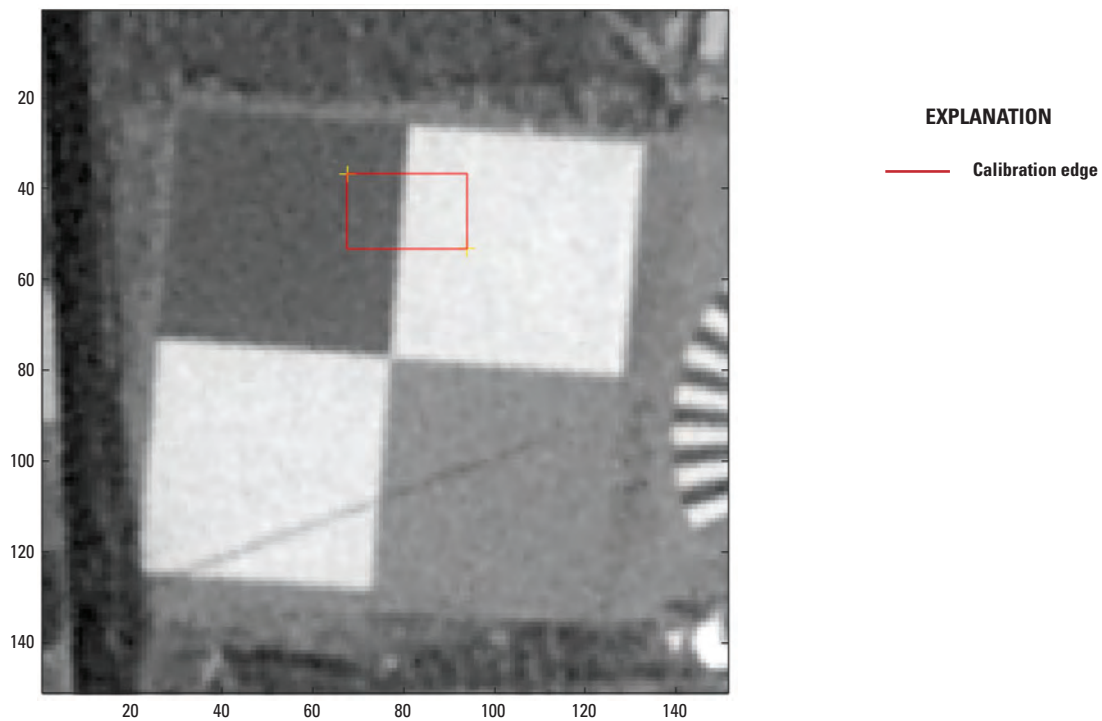


Figure 14. BlackSky image of calibration edge, Baotou, China.

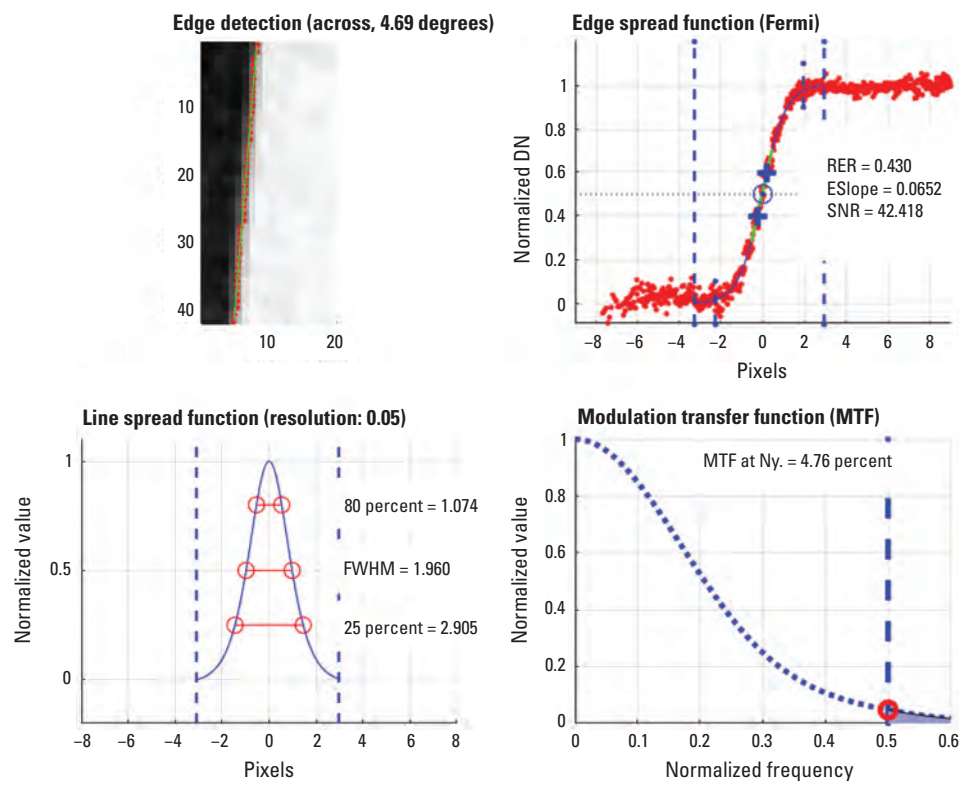


Figure 15. Edge detection, edge spread function plot, line spread function plot and modulation transfer function plot from the image quality estimation algorithm (based on Helder and others [2003]). [DN, digital number; RER, relative edge response; ESlope, slope of the line fit on the blue region of the edge spread function curve; SNR, signal to noise ratio; FWHM, full width at half maximum; Ny., Nyquist]

Table 10. Spatial performance of the BlackSky Global SpaceView-24 multispectral sensor using Innovative Imaging & Research, Inc., Image Quality Estimation software.

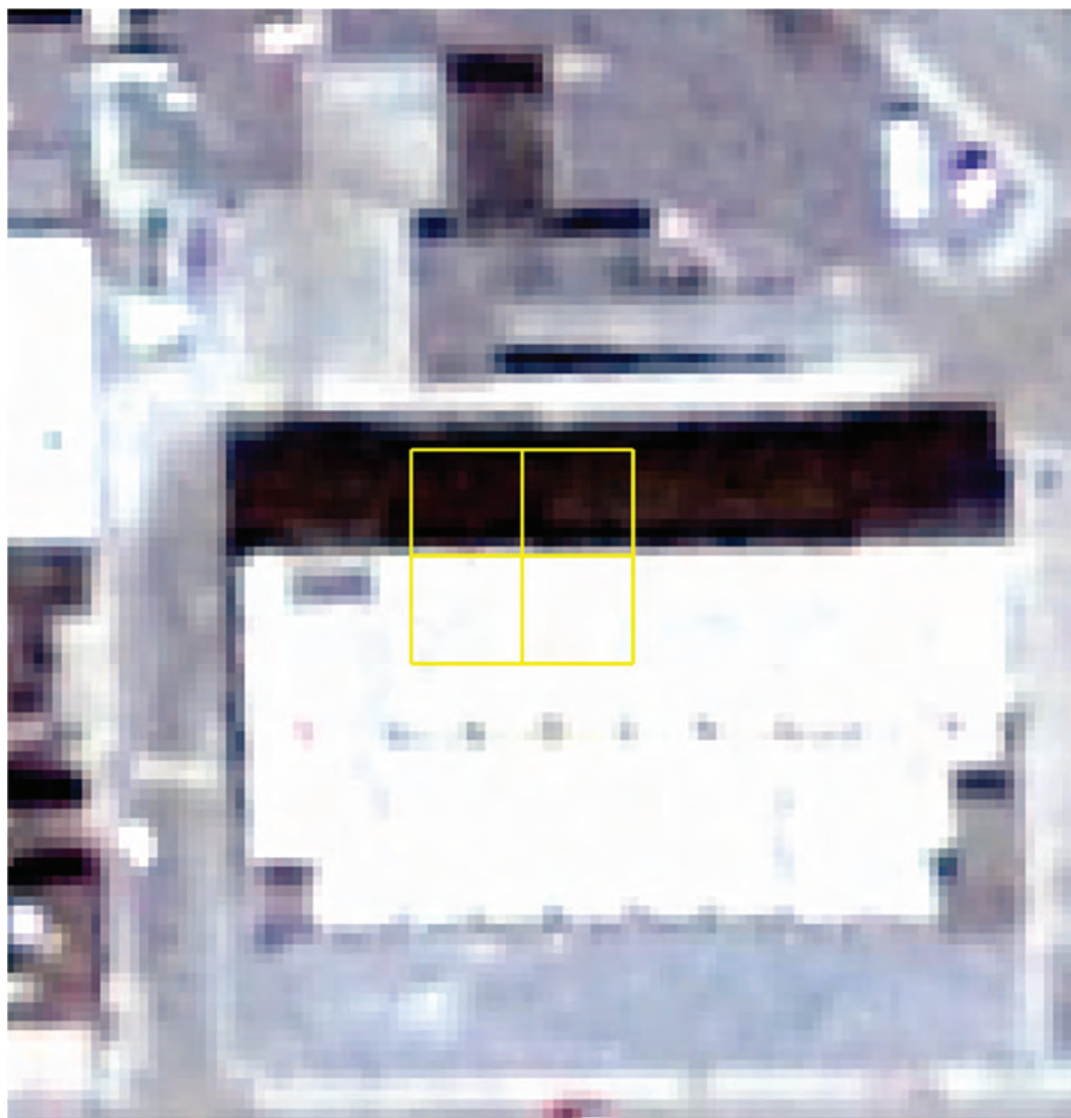
[RER, relative edge response; FWHM, full width at half maximum; MTF, modulation transfer function; %, percent]

Spatial analysis	RER		FWHM (pixels)		MTF at Nyquist (%)	
	Along	Across	Along	Across	Along	Across
Band 1—red	0.40	0.42	2.06	2.25	8.0	5.0
Band 2—green	0.41	0.43	1.99	2.01	5.0	6.0
Band 3—blue	0.47	0.43	1.98	2.09	8.0	5.0

Table 11. Spatial performance of the BlackSky Global SpaceView-24 multispectral sensor using U.S. Geological Survey Earth Resources Observation and Science system characterization software.

[RER, relative edge response; FWHM, full width at half maximum; MTF, modulation transfer function; %, percent]

Spatial analysis	RER	FWHM (pixels)	MTF at Nyquist (%)
Band 1—red	0.36	2.43	4.5
Band 2—green	0.38	2.35	6.0
Band 3—blue	0.41	2.25	7.4



EXPLANATION

— Calibration edge

Figure 16. BlackSky image of calibration edge, Sioux Falls, South Dakota.

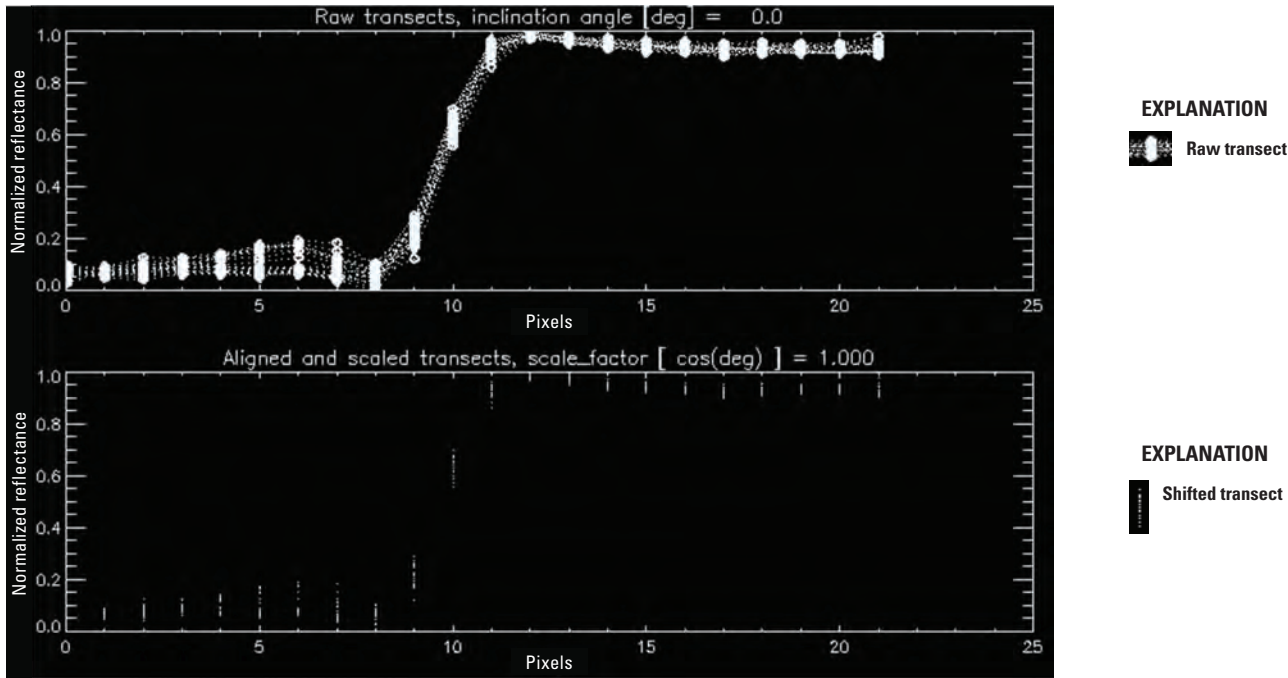


Figure 17. Band 1 raw edge transects (upper) and shifted transects (lower).

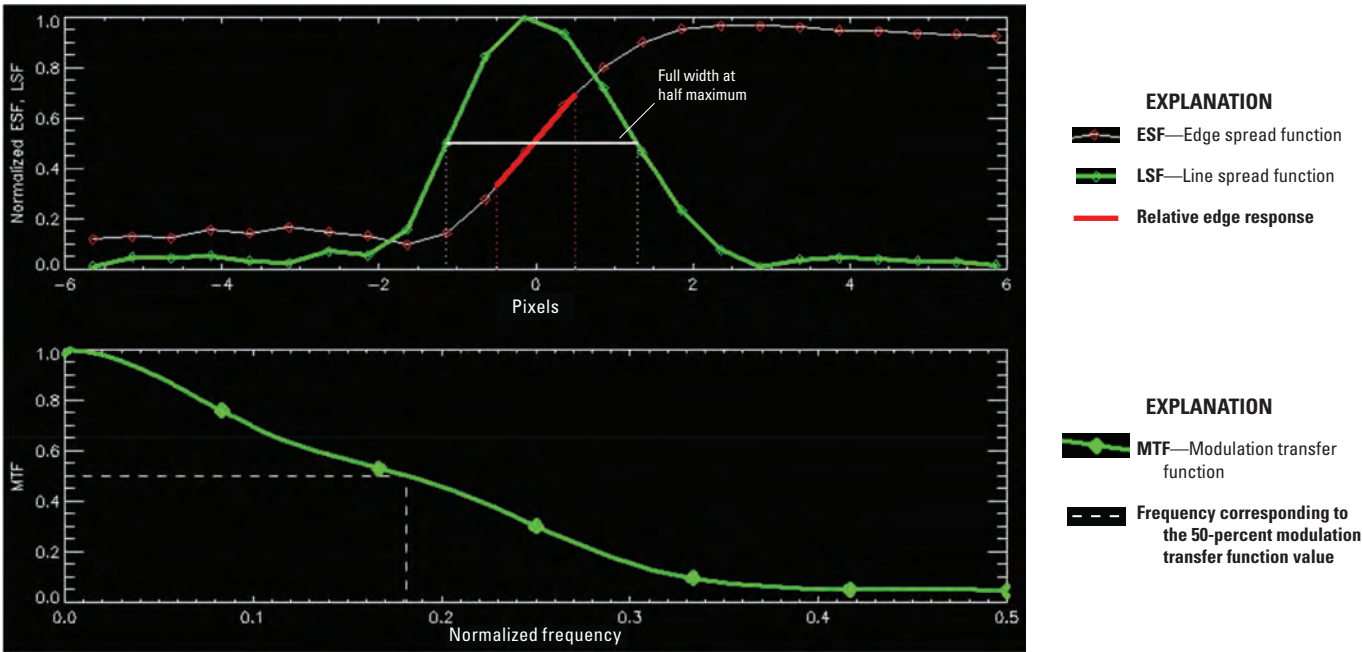


Figure 18. Band 1 edge spread function and line spread function (upper) and modulation transfer function (lower).

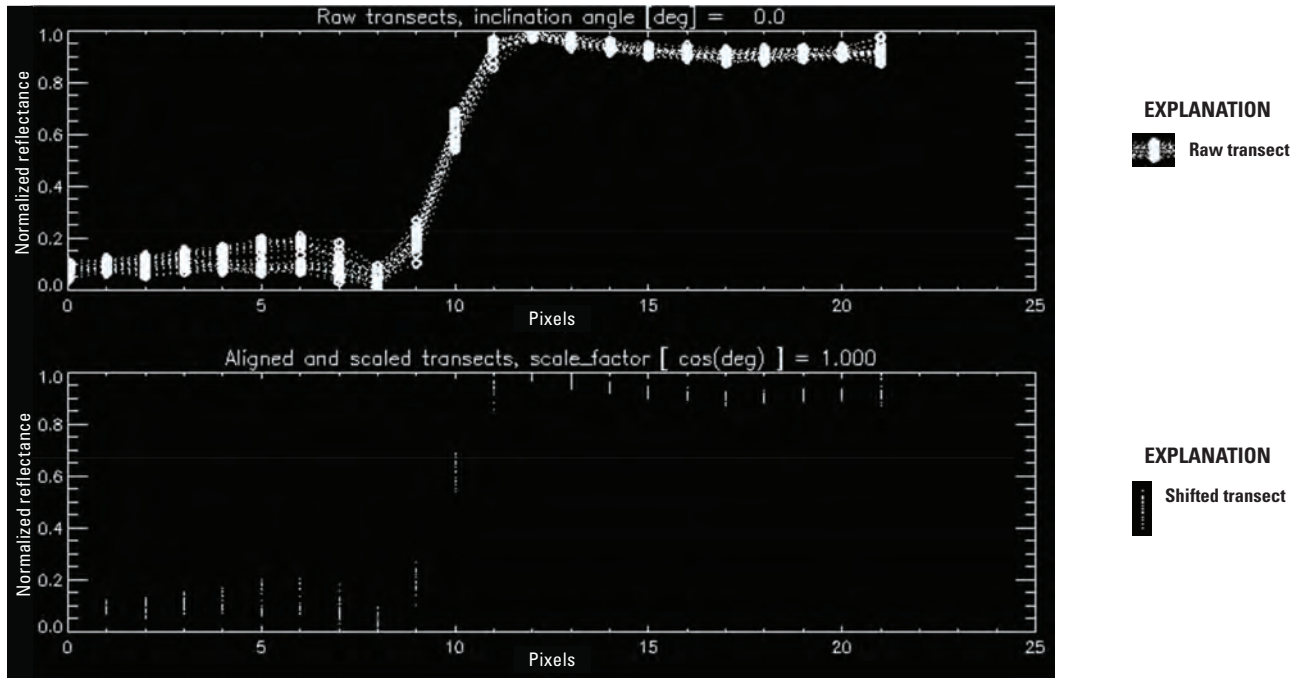


Figure 19. Band 2 raw edge transects (upper) and shifted transects (lower).

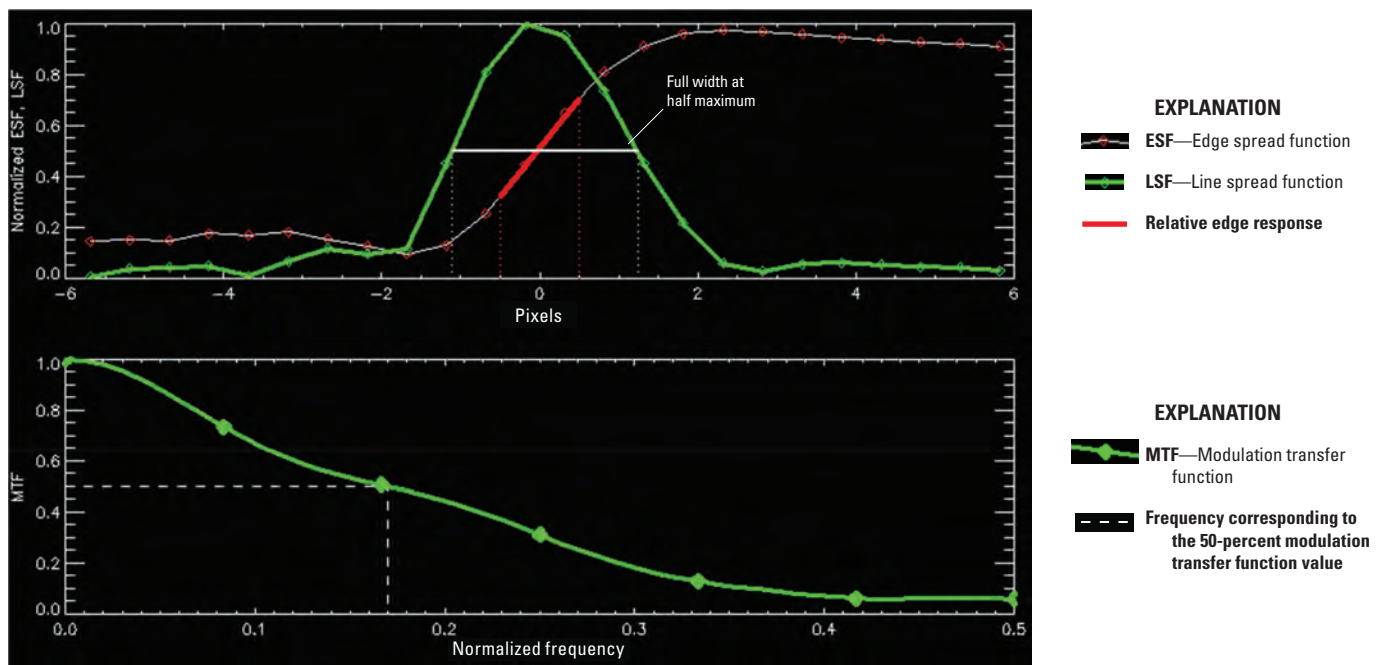


Figure 20. Band 2 edge spread function and line spread function (upper) and modulation transfer function (lower).

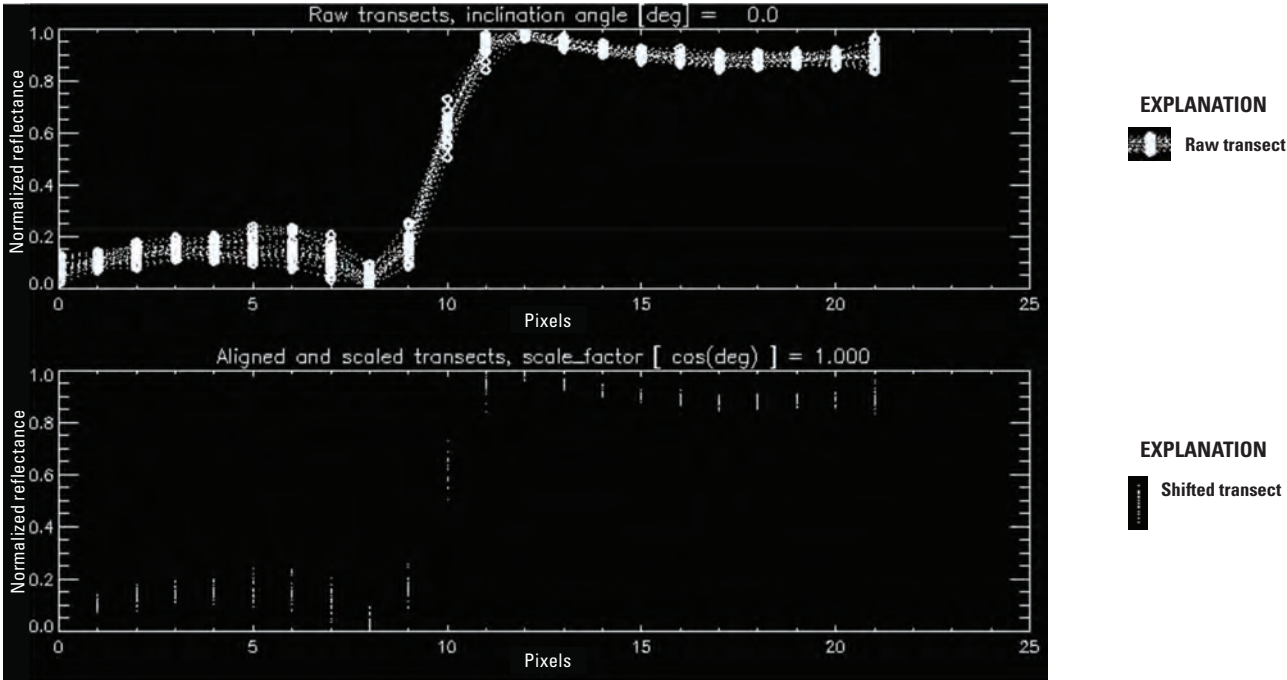


Figure 21. Band 3 raw edge transects (upper) and shifted transects (lower).

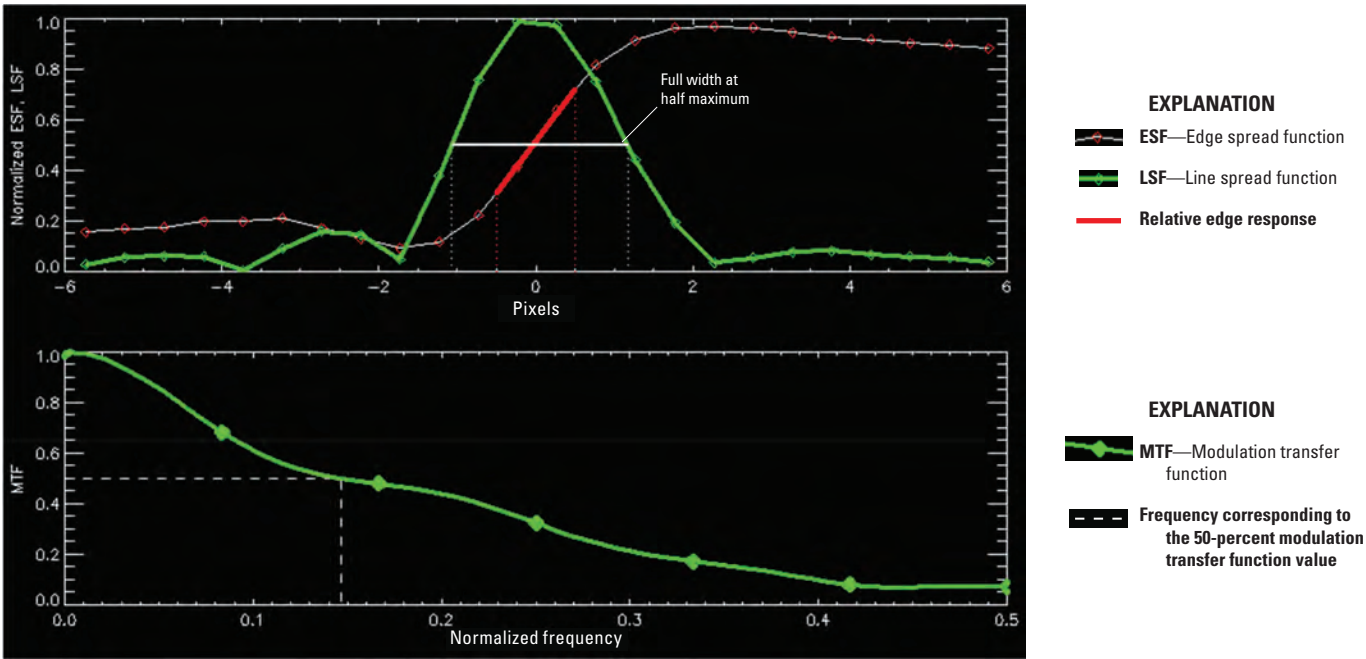


Figure 22. Band 3 edge spread function and line spread function (upper) and modulation transfer function (lower).

Summary and Conclusions

This report summarizes the sensor performance of the BlackSky Global satellites based on the U.S. Geological Survey Earth Resources Observation and Science CalVal Center of Excellence (ECCOE) system characterization process. In summary, we have determined that these sensors provide an interior geometric performance in the range of -0.011 meter (-0.012 pixel) to 0.007 m (0.008 pixel) in easting and -0.018 m (-0.020 pixel) to 0.012 m (0.013 pixel) in northing in band-to-band registration; an exterior geometric performance using ground control points of 8.0-m circular error (95-percent certainty) for orthorectified products and 8.8 to 14.3-m circular error (95-percent certainty) for nonorthorectified products, depending on the geolocation metadata used; and a spatial performance in the range of 1.70 to 2.43 pixels for full width at half maximum, with a modulation transfer function at a Nyquist frequency in the range of 0.032 to 0.084.

In conclusion, the team has completed an ECCOE standardized system characterization of the BlackSky Global satellites. Although the team followed characterization procedures that are standardized across the many sensors and sensing systems under evaluation, these procedures are customized to fit the individual sensor, as was done with the BlackSky Global satellites. The team has acquired the data, defined proper testing methodologies, carried out comparative tests against specific references, recorded measurements, completed data analyses, and quantified sensor performance accordingly. The team also endeavored to retain all data, measurements, and methods, which is key to ensure that all data and measurements are archived and accessible and that the performance results are reproducible.

The ECCOE project and associated Joint Agency Commercial Imagery Evaluation partners are always interested in reviewing sensor and remote sensing application assessments and would like to see and discuss information on similar data and product assessments and reviews. If you would like

to discuss system characterization with the U.S. Geological Survey ECCOE and (or) the Joint Agency Commercial Imagery Evaluation team, please email us at eccoe@usgs.gov.

Selected References

- Helder, D., Choi, T., and Rangaswamy, M., 2003, In-flight characterization of image spatial quality using point spread functions: ISPRS International Workshop on Radiometric and Geometric Calibration, Gulfport, Miss., December 2–5, 2003, 38-slide presentation.
- Innovative Imaging & Research, Inc., 2018, Image Quality Estimation user's guide: Stennis Space Center, Miss., Innovative Imaging & Research, Inc., 20 p.
- Ramaseri Chandra, S.N., Christopherson, J.B., Casey, K.A., Lawson, J., and Sampath, A., 2022, 2022 Joint Agency Commercial Imagery Evaluation—Remote sensing satellite compendium: U.S. Geological Survey Circular 1500, 279 p. [Also available at <https://doi.org/10.3133/cir1500>.] [Supersedes USGS Circular 1468.]
- U.S. Geological Survey, 2020a, EROS CalVal Center of Excellence (ECCOE): U.S. Geological Survey web page, accessed March 2021 at <https://www.usgs.gov/core-science-systems/eros/calval>.
- U.S. Geological Survey, 2020b, EROS CalVal Center of Excellence (ECCOE)—JACIE: U.S. Geological Survey web page, accessed December 2021 at https://www.usgs.gov/calval/jacie?qt-science_support_page_related_con=3.
- U.S. Geological Survey, 2020c, Landsat missions—Glossary and acronyms: U.S. Geological Survey web page, accessed March 2021 at <https://www.usgs.gov/core-science-systems/nli/landsat/glossary-and-acronyms>.

For more information about this publication, contact:

Director, USGS Earth Resources Observation and Science Center
47914 252nd Street
Sioux Falls, SD 57198
605-594-6151

For additional information, visit: <https://www.usgs.gov/centers/eros>

Publishing support provided by the
Rolla Publishing Service Center

